Available online at www.sciencedirect.com
ScienceDirect
Journal of the European Ceramic Society 28 (2008) 1433–1441
www.elsevier.com/locate/jeurceramsoc

Microstructural engineering of microwave dielectric ceramics

R. Freer*, F. Azough

Materials Science Centre, School of Materials, University of Manchester, Manchester M1 7HS, UK

Available online 25 January 2008

Abstract

Temperature stable, low loss dielectric ceramics find application as resonators in communication systems operating at microwave frequencies. Candidate materials need to exhibit high relative permittivity, high dielectric Q value and near zero temperature coefficient of resonant frequency. Current materials include a range of complex perovskites, predominantly titanate-based, with $Q \times f_o$ (product of Q value and resonant frequency) values of 250,000 GHz or more. An overview is given in the ways in which the microstructures of microwave dielectric ceramics have been 'engineered' at the levels of the grain, grain boundary, sub-grain and the lattice to optimise the critical dielectric parameters. This is primarily accomplished by either (a) modifying the processing conditions, or (b) modifying the powder formulation (from dopants to major compositional changes). The outcomes provide a series of ground rules to maximise the performance of new materials.

Keywords: Dielectric properties; Microwave dielectrics; Sintering; Perovskites

1. Introduction

Microwave dielectric ceramics are crucial components in mobile telephone systems. In the form of dielectric resonators they enable the filter units in the mobile telephone base stations to remove unwanted sidebands and secondary signals, ensuring transmission of high quality primary signals with minimum interference. The concept of using a solid dielectric as a resonator in place of the traditional air-filled metal cavity is generally attributed to Richtmyer[1] in 1939. The ceramic resonator offers significant advantages in terms of space saving and signal selectivity over the traditional structure. Based upon the original Richtmyer model, a monomode ceramic resonator is cylindrical in shape, with a central, axial cavity, allowing standing waves to be set up within the outer solid 'doughnut'. In spite of the simplicity of the solid resonator model, it was almost 30 years before the first ceramic resonators were realised[2] and a further decade[3,4] before high quality components became commonly available.

For a material to be considered as candidate for a microwave dielectric resonator, there are three critical requirements:

(i) The relative permittivity (ε_r) should be as large as possible, since the size of a resonator is inversely proportional to the square root of relative permittivity. In reality the range of materials is restricted to approximately $20 < \varepsilon_r < 100$, in order that other conditions can be met.
(ii) The dielectric losses ($\tan\delta$) should be as small as possible to ensure maximum signal discrimination. This is more commonly described in terms of the dielectric Q value ($1/\tan\delta$) which should be maximised. However, Q is not an independent parameter, as experience has shown[5] that for a given material the product of Q and the resonant frequency (f_o) is approximately constant (known as the figure of merit) and therefore statements on the Q value of a material should always refer to the measurement (resonant) frequency. For many practical applications today, $Q > 30{,}000$ at 1 GHz is essential.
(iii) To ensure temperature stability in communications systems, the resonator needs to have a temperature coefficient of resonant frequency (τ_f) $\sim \pm 2$ ppm/°C, so that the signal does not drift during device operation.

Titania (TiO_2) was one of the materials explored[6] for resonator applications in the 1960s. With a relative permittivity of ~100 and high Q value it immediately met criteria (i) and (ii), but failed the final criteria (iii) with very poor temperature stability ($\tau_f \sim +450$ ppm/°C). Since τ_f is linked to the temperature coefficient of relative permittivity (τ_ε) and the coefficient of thermal expansion (α_L) by

$$\tau_f = -\left(\frac{\tau_\varepsilon}{2+\alpha_L}\right) \quad (1)$$

* Corresponding author. Tel.: +44 161 306 3564; fax: +44 161 306 8877.
E-mail address: Robert.Freer@manchester.ac.uk (R. Freer).

0955-2219/$ – see front matter © 2007 Elsevier Ltd. All rights reserved.
doi:10.1016/j.jeurceramsoc.2007.12.005

then τ_f needs to be small, but non-zero to compensate for the thermal expansion of the resonator.[7]

Hence for the development of new and improved microwave dielectrics the objectives are (i) high or increased ε_r, (ii) high or increased $Q \times f_o$, and (iii) near zero τ_f. There are various strategies to achieve such changes in the materials, and here we will explore the potential offered by 'microstructural engineering'. In the case of ZnO varistors, where the non-linear electrical properties are controlled by the defect chemistry of the grain and the grain boundary regions, Gupta[8] applied the concept of 'microstructural engineering' through donor and acceptor doping of the grains and grain boundaries. He identified three levels of engineering the microstructure, in terms of (i) the types of dopants (grain/grain boundary specific), (ii) whether the dopant acts as donor or acceptor, and (iii) whether the dopant sits on a lattice or interstitial site. In the case of microwave dielectric ceramics we will consider four levels of engineering: the grain level, the grain boundary, the sub-grain, and the lattice (or point defect) level. To set this work in context, the following section provides a brief historical introduction.

2. Historical development

The earliest studies of resonator materials commenced with the work of Cohn[6] on titania in the 1960s (which exhibited high τ_f as noted above), but also included pioneering investigations by Bolton[2] on high permittivity tungsten bronze-structured $BaTiO_3$–Ln_2O_3–TiO_2, which achieved temperature stability and relative permittivities of 60–80. Negas et al.[9] noted that the work of Bolton is rarely acknowledged in subsequent literature, but provided the technical foundation for a host of investigations of tungsten bronze structure materials.

By the late 1970s and early 1980s there was interest in a range of materials including $MgTiO_3$–$CaTiO_3$, $(Zr,Sn)TiO_4$ and $BaTi_4O_9$. Plourde and Ren[10] in 1981 reported that the maximum $Q \times f_o$ available was around 36,000 GHz, with maximum ε_r of 40 (again overlooking the work of Bolton[2]). Data for typical microwave dielectric ceramics in 1981 are summarised in Table 1. The growth of the mobile communications market in the 1990s stimulated research in microwave dielectrics, particularly for high relative permittivity materials ($\varepsilon_r \sim 75$–90) for mobile telephone handset applications, and very high Q materials ($Q \sim 30{,}000$ at 3 GHz) for base station applications.[7] For the former group, the high ε_r tungsten bronze-structured materials (for example $BaTiO_3$–Nd_2O_3–TiO_2) remained the primary choice,

Table 1
Typical properties of microwave dielectric ceramics in 1981 (from references[2,9–11])

	ε_r	$Q \times f_o$ (GHz)	τ_f (ppm/°C)
$Ba_2Ti_9O_{20}$	40	36,000	+2
$(Zr,Sn)TiO_4$	34–37	36,000	∼20
$(Sc,Ca)\{(Li,Nb)Ti\}O_3$	36–46	38,000	+30 to −70
$BaTi_4O_9$	38	34,000	+15
$(Ca,Sr)\ (BaZr)O_3$	29–32	27,500	±50
$BaTiO_3$–Nd_2O_3–TiO_2	62–80	[a]	

[a] Properties measured at 1 MHz.

Table 2
Typical examples of temperature stable ($\tau_f \sim 0$) microwave dielectric ceramics available in 2007 (after Reaney and Iddles[7])

	ε_r	$Q \times f_o$ (GHz)
$BaMg_{1/3}Ta_{2/3}O_3$	24	250,000–300,000
$BaZn_{1/3}Ta_{2/3}O_3$	29	150,000
$Ba(Co,Zn)_{1/3}Nb_{2/3}O_3$	34	90,000
$SrTiO_3$–$LaAlO_3$	39	60,000
$CaTiO_3$–$NdAlO_3$	45	48,000
$ZrTi_2O_6$–$ZnNb_2O_6$	44	40,000–48,000
$Ba_{6-3x}R_{8+2x}Ti_{18}O_{24}$	80–90	7,000–13,000

whilst complex perovskites (for example $BaMg_{1/3}Ta_{2/3}O_3$, ε_r 24–29) provided the highest Q values for the base stations. Between these two families there was still a significant gap in terms of relative permittivities; the simple perovskites (for example $CaTiO_3$–$LaAlO_3$, ε_r ∼45) and the two-phase α-PbO_2-structured $ZrTiO_4$–$ZnNb_2O_6$ ($\varepsilon_r \sim 44$) with $Q \times f_o$ values around 48,000 GHz have gone some way for providing 'mid-range' materials. A summary of typical materials available in 2007 is presented in Table 2. A striking feature is still the gap in the available materials with ε_r in the range 45–75. Reaney and Iddles[7] highlighted the fact that materials with ε_r of 45–75, with high Q value and zero τ_f do not currently exist. The following sections examine ways in which the microstructures of microwave dielectric ceramics have been 'engineered' *at different levels* to optimise the critical dielectric parameters. The outcomes provide a series of ground rules to maximise the performance of new materials. They may ultimately provide a way forward to develop materials with both high Q and high ε_r in the permittivity 45–75 gap.

There are two principle routes to engineer the microstructure, either (a) modifying the processing conditions, or (b) modifying the powder formulation (from dopants to major compositional changes). Both are relevant to microwave dielectric ceramics and achieve effects at different levels.

3. Engineering at the grain level

For a given formulation the optimum relative permittivity can be achieved by maximising density and eliminating porosity, as for all ceramics. If the base composition is itself not temperature stable, then cations can be substituted, until $\tau_f \sim 0$ is achieved. When the substitution gives rise to an increase in polarizability, then there is further benefit of an increase in relative permittivity as well. For example $MgTiO_3$ and $CaTiO_3$ have very different properties; $MgTiO_3$ has negative τ_f (−45 ppm/°C), low ε_r (17) and high Q (22,000 at 7 GHz), whilst $CaTiO_3$ has a large positive τ_f (+800 ppm/°C) high ε_r (170), and low Q (1800 at 7 GHz). When they are combined in the ratio $MgTiO_3$:$CaTiO_3$ of 95:5, then a temperature-stable dielectric is achieved, which has a higher ε_r (21) than the base $MgTiO_3$, but a Q value (8000 at 7 GHz) which is inevitably lower than that of the pure $MgTiO_3$.

The possibility of combining two dielectrics of different relative permittivity or temperature dependence to obtain a material with the desired properties has long been known. There are many empirical relationships to describe the interaction of two

components and the predicted properties of the product. The Liechtenecker logarithmic rule relates the volume fractions (x and $1-x$) and the relative permittivities ε_1 and ε_2 of the two components to the final relative permittivity ε':

$$\log \varepsilon' = (1-x)\log\ \varepsilon_1 + x\ \log\ \varepsilon_2 \quad (2)$$

The equivalent relationship for the temperature dependence of relative permittivity (τ_ε) for a material resulting from components (1) and (2) is:

$$\tau_\varepsilon = (1-x)\tau_\varepsilon(1) + x\,\tau_\varepsilon(2) \quad (3)$$

These relationships have proved very useful in designing materials, but occasionally the materials do not follow the predictions. The system $AgNbO_3$–$AgTaO_3$ (ATN) exhibits complete solubility, but the end members exhibit opposite temperature dependencies of permittivity; Volkov et al.[12] reported that $AgNbO_3$ has a strongly positive τ_ε and $AgTaO_3$ strongly negative τ_ε. Valant et al.[13] anticipated that by combining the two components a temperature-compensated dielectric would be achieved. In fact the mid-range composition $AgNb_{0.5}Ta_{0.5}O_3$ exhibited τ_ε of +1300 ppm/°C below 60 °C and −1200 ppm/°C above 60 °C. Adjusting the Nb to Ta ratio in $AgNb_xTa_{1-x}O_3$ did not suppress the strong temperature dependence. Valant et al.[13] then explored an alternative strategy of sintering chemically non-compatible phases; this involved the formation of two-phase ceramics, with the minimum possible interaction between the two phases. They initially prepared the two phases separately ($AgNbO_3$-rich and $AgTaO_3$-rich) and then formed (i) mixtures of fine powders of ~1 μm in size, (ii) mixtures of coarse powders 20 μm in size, and (iii) mixtures of coarse granulates ~100 μm in size. Each was pressed and sintered. In fact the ceramics prepared from the granulates (case iii) exhibited the optimum temperature dependence (Fig. 1), although the individual granulates contained higher levels of porosity than products from either (i) or (ii).

In cases where the powder formulation is fixed, then there are occasions where the phases present evolve during processing and this can have a significant effect on properties. For example the complex perovskite $Ba(Zn_{1/3}Nb_{2/3})O_3$ (BZN) has a relative permittivity of 40, a $Q \times f_o$ of >60,000 and a τ_f of +20 ppm/°C. This has provided the base material for a range of high Q resonator materials in the past decade. During sintering at temperatures up to 1550 °C, there is loss of the volatile Zn from the outer edges of the ceramic, leading to the formation of Zn-deficient phases.[14] Fig. 2 shows the microstructure of a $Ba(Zn_{1/3}Nb_{2/3})O_3$ ceramic exhibiting three distinct phases. The core of the sample is the primary $Ba(Zn_{1/3}Nb_{2/3})O_3$ phase; adjacent to it is a Zn-deficient phase, $Ba_8ZnNb_6O_{24}$ (so called 8-1-6-24 phase), and the outermost phase is the needle-shaped grains of Zn-free $Ba_5Nb_4O_{15}$. Whilst the total volume of these Zn-poor phases is not more than 1–2% of the ceramic, the presence of these additional phases appears to be beneficial, since removal of them tends to degrade the dielectric properties. Both the additional phases have similar relative permittivities to the primary phase, and the 8-1-6-24 phase has moderate Q value ($Q \times f_o > 56{,}000$) and a positive τ_f (+35 ppm/°C); the Zn-free

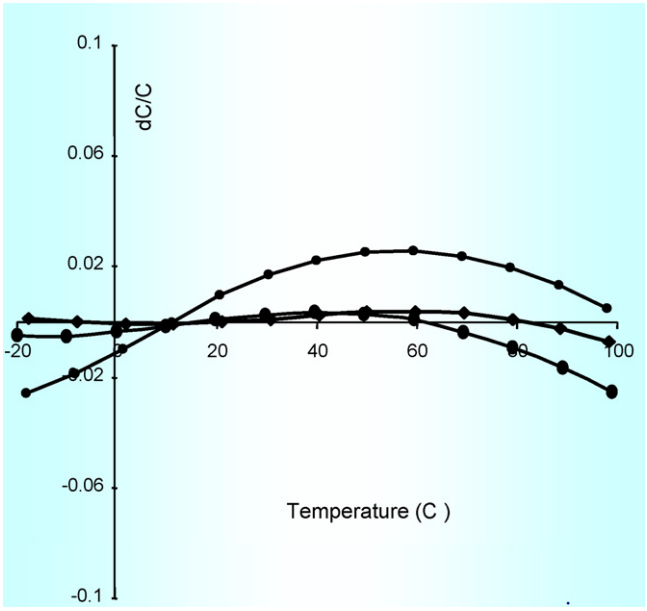

Fig. 1. Temperature dependence of permittivity of ceramics of mixed $AgNbO_3$–$AgTaO_3$ ceramics: (●) milled powder; (⬟) hand-ground powder; (♦) large granulates (after Valant et al.[13]).

$Ba_5Nb_4O_{15}$ is a high Q material ($Q \times f_o = 52{,}000$) with τ_f of +70 ppm/°C.

Finally at the grain level, the role of internal stress and structural imperfections should not be overlooked. With $MgTiO_3$ Ferreira et al.[15] showed that chemical processing enabled the Q value to be increased from 9000 at 8 GHz (for mixed oxide processing) to 21,000 GHz for specimens pressed isostatically. In contrast when chemically prepared powders were uniaxially pressed the maximum Q value was 9800 GHz for samples sintered under the same conditions. It is generally assumed that sintering at high temperature removes strains generated by pressing, but clearly with some powder system lubricants and other additives may be required if sintering/annealing periods are short.

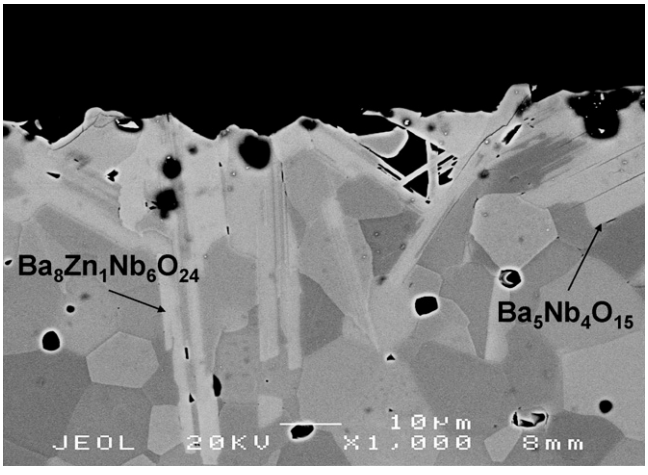

Fig. 2. Backscattered secondary electron SEM image of $Ba(Zn_{1/3}Nb_{2/3})O_3$ showing Zn-deficient phases near the outer edge of the sample.

4. Engineering at the grain boundary level

For many years there was speculation that the grain boundary region could have a significant effect on Q values.[9] Taking $Ba_2Ti_9O_{20}$ (B2T9) as an example Negas et al.[9] noted that the general feeling was that wider, 'dirty' boundaries, perhaps dominated by defects would cause lower Q values, whilst narrow, 'clean' boundaries were preferred. Early high-resolution TEM studies of the grain boundaries of microwave dielectrics[16] did little to resolve the questions concerning the origin of dielectric loss, but did still point to impurities as the primary source of extrinsic loss. In the case of $Ba_2Ti_9O_{20}$ there was a suggestion[16] that polytypic intergrowths inside the grains had an impact on the concentration of intrinsic defects. As a consequence there is a general strategy of aiming for clean grain boundaries to minimise the number of extrinsic defects. This usually means employing the highest purity starting powders (commensurate with cost) or leaching to clean the powders[4] and avoiding impurities and contamination during processing. All powders for bulk operations tend to contain very small levels of impurities, some of which may have deleterious effects on Q values. Wakino et al.[17] demonstrated that the presence of 0.2 wt% Fe_2O_3 in the starting powders for (Zr,Sn)TiO_4 (ZTS) reduced the Q value (at 7 GHz) from 8000 to ~2000, and that at 0.5 wt% Fe_2O_3 the Q value fell to 400 (Fig. 3). It was believed that the Fe^{3+} ions entered the primary grains in the ceramic, replacing one or more of the four-valent species, leading to the generation of oxygen vacancies. The net effect was major changes in the lattice vibrations and a reduction in the Q value. Somewhat surprisingly Wakino et al.[17] found that by adding controlled amounts of NiO (around 0.5 wt%) to the starting mixture (which already contained Fe_2O_3) the deterioration in Q value could be reduced to manageable levels, providing the ferric oxide was not at excessively high concentrations. In Fig. 3 it can be seen that when NiO is added, the deleterious effect of Fe_2O_3 on (Zr,Sn)TiO_4 is almost neutralised for ferric oxide concentrations up to 0.5 wt% (the same as the amount of NiO). The explanation for this behaviour is that the added NiO combines with the Fe_2O_3 already present in the powder to form a $NiFe_2O_4$ spinel phase in the grain boundaries. Trapping the Fe^{3+} at the grain boundaries prevents the ferric ions entering the primary grains and thereby forming defects. Whilst the spinel phase has a low dielectric Q value, the volume of this second phase is very small and therefore the effect on the Q value is negligible.[17]

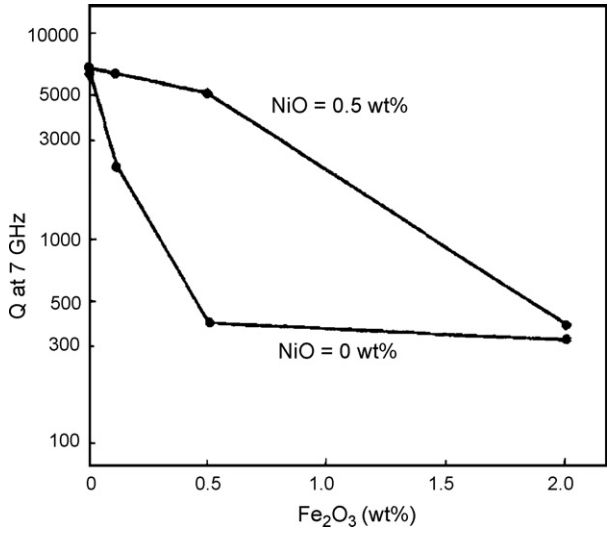

Fig. 3. Effect Fe_2O_3 and NiO additives on the dielectric Q value of (Zr,Sn)TiO_4 ceramics (after Wakino et al [17]).

5. Engineering at the sub-grain level

Domains are important sub-grain features and are found extensively in materials which undergo structural transitions after sintering. $CaTiO_3$-based materials are usually sintered at temperatures of ~1400 °C, and transform upon cooling from cubic to tetragonal at 1307 °C, and then to orthorhombic at 1227 °C. Fig. 4 shows a typical TEM microstructure of $CaTiO_3$ after sintering at 1400 °C followed by cooling at 6 °C h^{-1}. There is a high density of twins inside each grain; TEM analysis enabled the twin domains to be classified according to the symmetry elements at the twin boundaries as {1 1 2} and (1 1 0) twin types.[19] By cooling samples at different rates after sintering (air quench to 1 °C h^{-1}) it was possible to generate a range of microstructures and domain densities. From orientation contrast maps[20] (obtained by electron backscatter diffraction, EBSD) the domain densities were determined. The quenched samples were characterised by small grain size ~5 μm, a high density of twins within the grains and a high number of needle-like twins. When the samples were cooled at 6 °C h^{-1}, the average grain size increased ~10 μm, the number of twins per unit area decreased (by about 30%), and there was a significant reduction in the number of needle-like twins. The slowly cooled samples are also associated with a higher Q value than the quenched samples. Whilst it is not possible to isolate the effect of the density of twin domains from other factors in this example (since the samples effectively spent different times at elevated temperature) there is strong circumstantial evidence to suggest that a lower density of twin domains is associated with higher Q values.

An alternative approach, avoiding differential or extended annealing periods, is to add a phase which promotes

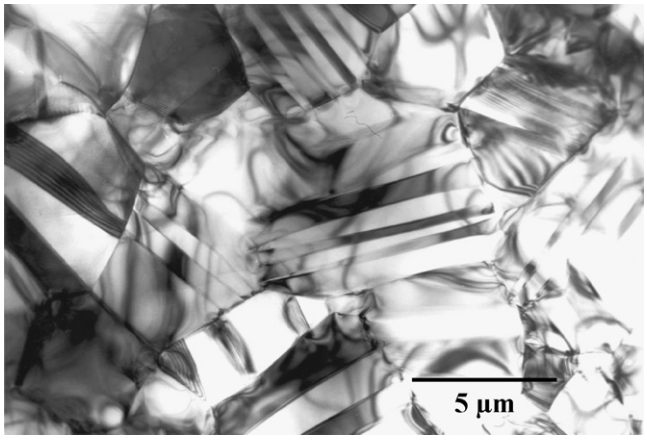

Fig. 4. TEM image showing twins in single grains in $CaTiO_3$ ceramic, sintered at 1400 °C (after Kipkoech et al.[18]).

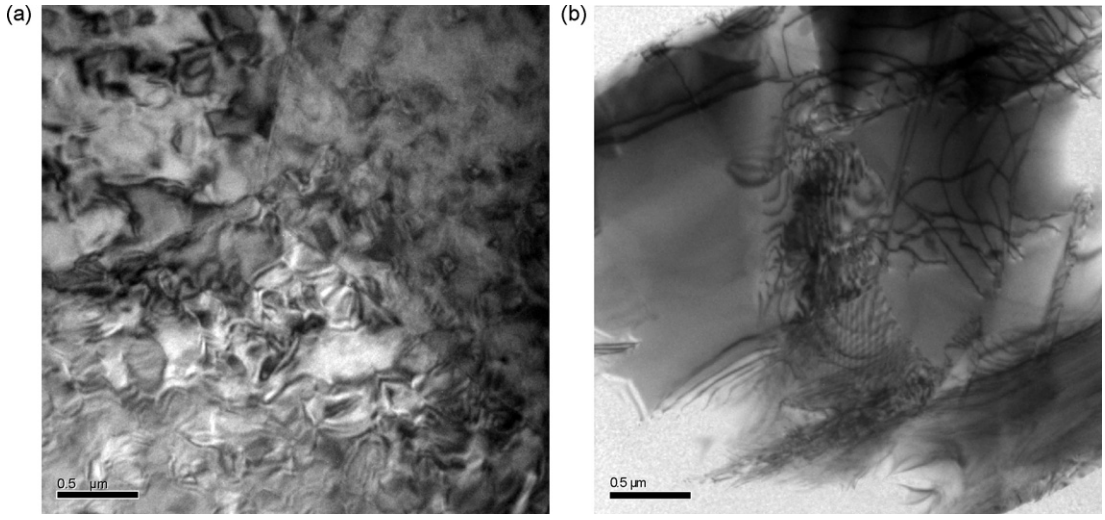

Fig. 5. TEM images of (a) $Ba(Zn_{1/3}Nb_{2/3})O$ ceramic, and (b) $Ba(Zn_{1/3}Nb_{2/3})O$ prepared with additions of 8-1-6-24 phase.

domain (and possibly grain) growth. The normal sintering of $Ba(Zn_{1/3}Nb_{2/3})O_3$ (BZN) gives rise to surface phases deficient in Zn, which exhibit very different microstructures to that of the host perovskite (Fig. 2). By preparing BZN powder batches containing a few mole percent of added $Ba_8ZnNb_6O_{24}$ (the 8-1-6-24 phase) the products are distinctly two phase, but dominated by the primary BZN perovskite. The most obvious difference from the standard material is the significant increase in grain size, in some cases by a factor of five. TEM investigations revealed dramatic differences in the domain structures. In the conventional BZN material there is a multi-domain structure within each of the (small) grains (Fig. 5a). In contrast, in the BZN prepared with the 8-1-6-24 phase, the large grains are essentially monodomain, with dislocations the only obvious features (Fig. 5b). Again the reduction in domain density is associated with higher Q values.

6. Engineering at the lattice level

Effects that may be engineered at the lattice level give rise to changes in either the Q value, or the temperature dependence of resonant frequency (τ_f). For convenience these will be considered separately.

6.1. Changes to the Q value

It was noted in the introduction that the product of the Q value and the resonant frequency ($Q \times f_o$) is approximately constant. This follows directly from classical dispersion theory[21] which predicts that at microwave frequencies, relative permittivity is independent of frequency and $\tan\delta$ is directly proportional to frequency (f) since

$$\tan\delta = \left(\frac{\gamma}{\omega_T^2}\right) f \tag{4}$$

where γ is the damping factor and ω_T is the resonant frequency of the optical mode of the lattice vibration. Hence Q decreases with increasing frequency.[5] Furthermore, the damping factor depends mainly on the effect of anharmonic terms in the potential energy associated with a pair of atoms,[21] and therefore the crystal structure effectively controls the intrinsic losses of the dielectric. Spitzer et al.[22] and Perry et al.[23] interpreted Fourier transform infrared spectra (FTIR) for perovskites in terms of classical dispersion theory. Subsequently Tamura et al.[24] used simple oscillator models to predict the *intrinsic* relative permittivity and Q value of $Ba(Zr,Ta)O_3$ (BZT) via dispersion parameters obtained from FTIR and Raman spectra[25]:

$$\varepsilon = \varepsilon_\infty + \sum_j 4\pi\rho_j \tag{5}$$

$$\tan\delta = \frac{\sum_j 4\pi\rho_j(\gamma_j\omega)/\omega_j^2}{\varepsilon_\infty = \sum_j 4\pi\rho_j} \tag{6}$$

where the strength $4\pi\rho_j$, width γ_j, and resonant frequency ω_j of each oscillator are the dispersion parameters and ε_∞ is the relative permittivity resulting from electronic polarisation at the higher frequencies. There was good agreement between the experimental and calculated values for BZT (~30), but the experimental Q value 9800 (at 7 GHz) was significantly less than the calculated value of 20,200 GHz, reflecting the fact that the sample contained extrinsic defects. Whilst there are clear explanations for the way that intrinsic dielectric parameters can be extracted from IR spectra,[25,26] all samples will contain significant levels of extrinsic defects, and the best that microstructural engineering can offer is to minimise the effects of such defects.

Over two decades ago Kawashima et al.[27] examined the effect of annealing time on BZT samples, by sintering at 1350 °C for periods of 2–120 h. As the anneal period increased there was distinct splitting of the (2 2 6) and (4 2 2) X-ray diffraction peaks, reflecting the development of B-site ordering (Zr,Ta); this was accompanied by an increase in the Q value, achieving a maximum of 14,000 at 12 GHz. Other early documented examples of the increase in the Q value with cation ordering in perovskites included the work of Tamura et al.[28] on $Ba(Zr,Ta)O_3$–$BaZrO_3$, and Matsumoto et al.[29] on $Ba[(Mg,Co)_{1/3}Nb_{2/3}]O_3$. Fig. 6 shows X-ray diffraction data for $Ba[(Co,Zn)_{1/3}Nb_{2/3}]O_3$ as a function

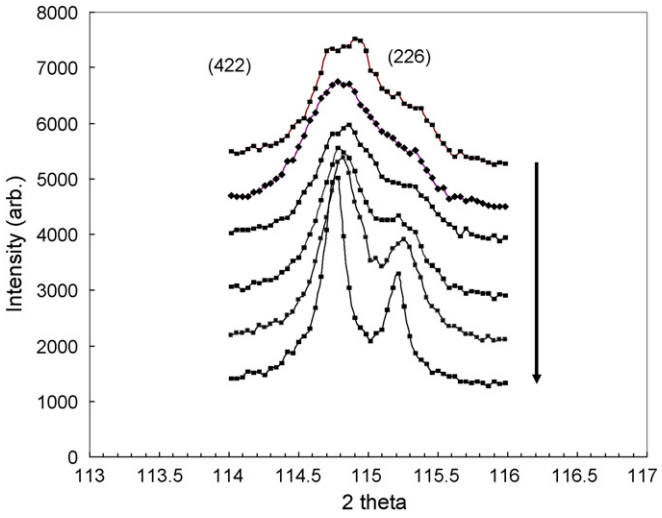

Fig. 6. Effect of annealing time on the development of ordering in $Ba[(Co,Zn)_{1/3}Nb_{2/3}]O_3$ ceramic, highlighted by the change in the intensity and the separation of (4 2 2) and (2 2 6) peaks (annealing time increases in the direction of the arrow: 0, 4, 12, 24, 48, 120 h).

of sintering time. For times greater than 12 h there is clear splitting of the (2 2 6) and (4 2 2) peaks; the separation is particularly obvious for the samples annealed for 48 and 120 h. With increasing sintering time the $Q \times f_o$ value increased from 45,000 to 50,000 GHz (0–4 h) to 85,000 GHz, for times $\geq$24 h. This was accompanied by an increase in the size of the domains from ~40 Å to 200–300 Å over the same time range. In the related material $BaMg_{1/3}Ta_{2/3}O_3$, $Q \times f_o$ values of 250,000 GHz are achievable with careful processing (Table 2) and by extended annealing, values in excess of 300,000 GHz are attainable. Fig. 7 shows HRTEM image of a high Q $BaMg_{1/3}Ta_{2/3}O_3$ ceramic.

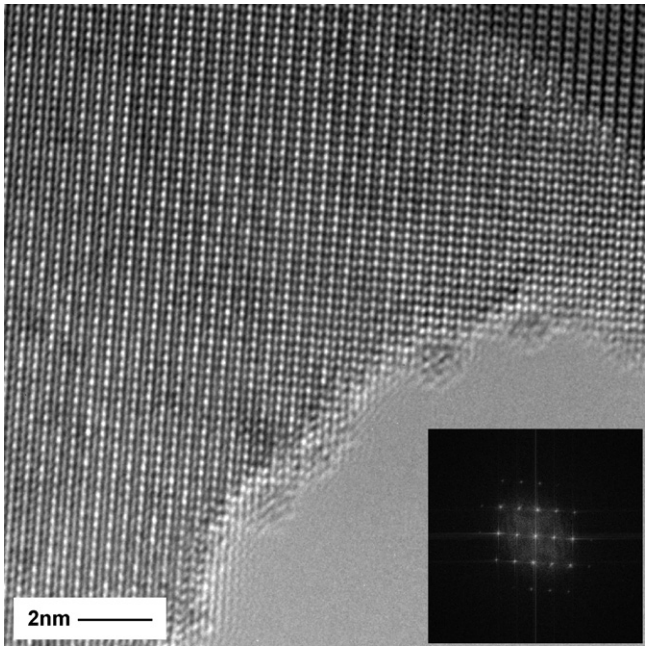

Fig. 7. HRTEM images of $BaMg_{1/3}Ta_{2/3}O_3$; each ceramic grain comprises a single domain. The fast Fourier transform (FFT) of the image confirms the ordering in just one set of (1 1 1) planes of the cubic parent phase.

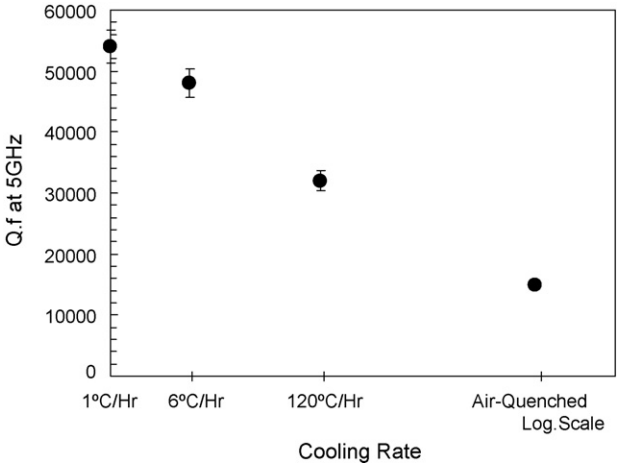

Fig. 8. $Q \times f_o$ value for $Zr_{0.8}Sn_{0.2}TiO_4$ as a function of cooling rate (after Azough and Freer[31]).

Ordering has developed to such a stage that each grain is equivalent to a single domain; the ordering occurs in just one set of (1 1 1) planes of the cubic parent phase.

Whilst there is a considerable volume of data on the effect of ordering in complex perovskites, ordering effects have also been reported in orthorhombic zirconium titante-based materials. Azough and Freer[30] prepared $Zr_{0.8}Sn_{0.2}TiO_4$ (which exhibits τ_f ~0); from standard laboratory grade powders. The products were sintered at 1400 °C and cooled at different rates, air quench to 1 °C h^{-1}. For rapid cooling rates, quite modest $Q \times f_o$ values were achieved, ~15,000–30,000 GHz. However, with slower cooling rates, the samples spend more time at elevated temperatures, and $Q \times f_o$ values up to 54,000 GHz were achieved (Fig. 7). The latter values are comparable with results obtained for high quality starting powders.[31] Azough and Freer[30] showed with X-ray diffraction and TEM data that the increase in Q value (Fig. 8) was associated with an increase in cation (Zr,Sn) ordering. Subsequent HRTEM studies of $ZrTiO_4$–$Zr_5Ti_7O_{24}$ solid solutions by Christofferson and Davies[32] revealed that as the structures change from disordered α-PbO_2 to more ordered forms, the structural arrangements appeared to be more complex than those found in complex perovskites. Within individual samples there were regions which exhibited layers of either Zr–Zr–Ti–Ti or Zr–Ti–Ti–Zr–Ti–Ti sequences in close proximity; frequently there were abrupt changes in occupancy of cation layers from predominantly Zr-rich to more Ti-rich. Nevertheless, the net increase in cation ordering is associated with higher Q values.

The potential problem of the reduction of Ti and the development of darkened cores in Ti-bearing ceramics during processing is well established. The problem tends to be more severe with large components and ceramics sintered in oxygen poor atmospheres. In high-density products, once the outer regions of the ceramic sinter, they effectively provide a seal, preventing oxygen transport to the core, exacerbating the reduction problem. Templeton et al.[33] identified a number of defect mechanisms by which the reduction of Ti (in TiO_2) could occur, involving the development of either oxygen vacancies or titanium interstitials, and possibly electronic conduction. The presence of vacancies in the lattice tends to reduce the vibration frequency, dampening the

phonon modes, and reducing the Q value. A simplistic solution to the reduction problem is to sinter samples in an oxygen-rich atmosphere, which may not be economically acceptable. For $Ba_2Ti_9O_{20}$ Nomura et al.[34] and Negas et al.[35] demonstrated that high Q values could be attained consistently in such titanates by acceptor doping with manganese. This allows charge compensation by the reaction: $Mn^{2+} + Ti^{4+} \leftrightarrow Mn^{3+} + Ti^{3+}$. Templeton et al.[33] subsequently examined the effects of 20 different dopants on the dielectric properties of TiO_2 ceramics. The reduction of Ti was prevented only when the titania was doped with divalent and trivalent ions which had an ionic radius within the range 0.5–0.95 Å; under such conditions favourable compensation mechanisms (like that for Mn) are believed to occur.

A related problem to the reduction of Ti is the generation of oxygen vacancies by the presence of impurities. In the case of (Zr,Sn)TiO_4 (ZTS) it was noted that Wakino et al.[17] found a substantial reduction in the Q value when Fe^{3+} was present in the starting powder (Fig. 3). Iddles et al.[36] suggested that the trivalent Fe substitutes for a quadrivalent ion, leading to the formation of oxygen vacancies. In terms of standard Kroger–Vink notation, this may be described as

$$Fe_2O_3 \rightarrow 2Fe'_{Zr} + 3O^x_o + V^{\bullet\bullet}_0 \quad (7)$$

The presence of Fe^{3+} causes the Q value (at 7 GHz) to fall from 6600 to 2700 GHz (Fig. 3). Iddles et al.[36] argued that addition of Nb_2O_5 to a powder already containing small amounts of Fe_2O_3 could be beneficial. When Nb_2O_5 is present on its own in (Zr,Sn)TiO_4, then potentially electron conduction could result:

$$Nb_2O_5 \rightarrow 2Nb^{\bullet}_{Zr} + 4O^x_o + \tfrac{1}{2}O_2 + 2e' \quad (8)$$

However, when Nb_2O_5 is added to a powder containing Fe_2O_3 impurities, then the proposed reaction[36] is

$$Fe_2O_3 + Nb_2O_5 \rightarrow 2Fe'_{Zr} + 2Nb^{\bullet}_{Zr} + 8O^x_o \quad (9)$$

Hence the Fe impurity in the powder is effectively neutralised and in fact Iddles et al. found that the Q value increase to 7000 GHz, higher than that for samples prepared with the nominally pure starting material.

6.2. Changes to τ_f

Substitution of cations can lead to major changes in relative permittivity, for example in $MgTiO_3$–$CaTiO_3$ (Section 3), but there are also opportunities to adjust the τ_f by compositional changes. From an empirical perspective, combining, in the correct proportions, two ceramics which exhibit positive and negative τ_f should yield a temperature stable material. Hence any substitution which affects τ_f will also modify the relative permittivity if the local polarizability is changed. Harrop[37] was the first to draw attention to the empirical, almost linear, relationship between τ_f and relative permittivity for $CaTiO_3$-based ceramics (also reviewed by Reaney and Iddles[7]) but Colla et al.[38] provided a physical explanation for τ_f changes in terms of the onset of octahedral tilt transitions. The latter relates to whether the corner sharing oxygen octahedra in the perovskite structure rotate either in-phase or anti-phase around the major axes.[7] The tolerance factor (t) is a very convenient way of assessing structural distortion caused by cation substitutions:

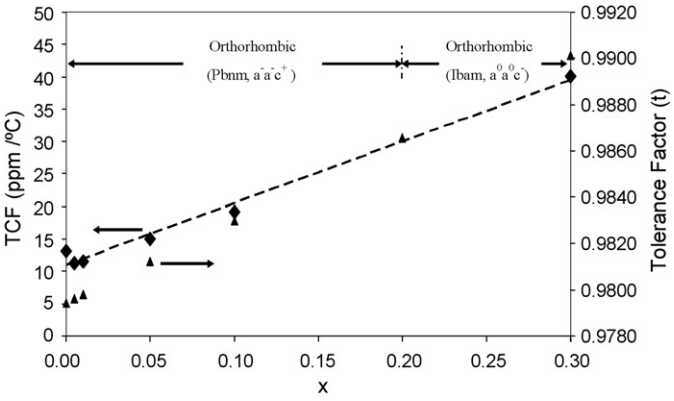

Fig. 9. Structural data for $Ca_{0.7-x}Sr_xTi_{0.7}La_{0.3}Al_{0.3}O_3$ ceramics as a function of Sr substitution (from unpublished work of Ravi[40]).

$$t = \frac{R_A + R_O}{\sqrt{R_B + R_O}} \quad (10)$$

where R_A, R_B and R_O are the atomic radii of A, B and O ions in the structure. At $t = 1$ there is a perfect match between the cation sizes in the perovskite framework and composition-induced lattice strain in the structure is virtually zero. As the tolerance factor deviates from unity, the mismatch between the A-site and B-site cations increases, inducing larger lattice stresses between critical ions and their neighbours in the perovskite framework.

Reaney et al.[39] identified a grossly non-linear relationship between τ_f and t for complex perovskites $A(B'B'')O_3$ (where A = Sr and Ba; B' = In, Ca, Co, Ni, Zn, Mg, Nd, Gd, and B'' = Ta or Nb) which correlated well with the tilt system present in the material. They postulated that the t value controls the temperature of onset of the tilt transitions and therefore τ_f. Three regions were identified in their summary diagram: (i) large positive τ_f, small t (0.92 to ~0.96) where there was anti-phase and in-phase tilting; (ii) large positive or large negative τ_f with mid-range t (~0.96 to 0.985) and anti-phase tilting; (iii) large positive τ_f, large t (0.985–1.06) and untilted structures. These relationships provide a very useful framework to explore the effect of substitutions in the perovskite structure and predict τ_f on the basis of t values. Fig. 9 shows data[40] for the relationship between τ_f, t and the tilt system in $Ca_{0.7-x}Sr_xTi_{0.7}La_{0.3}Al_{0.3}O_3$; with increasing Sr substitution there is an increase in τ_f, an increase in tolerance factor, and above a substitution level of $x = 0.20$ a change of tilt system from $a^-a^-c^+$ to $a^oa^oc^-$ in the notation defined by Glazer.[41]

7. Conclusions

From the examples considered it is clear that the microstructures of microwave dielectric ceramics can be engineered at different levels by either (a) modifying the powder formulation (from dopants to major compositional changes), or (b) modifying the processing conditions. Table 3 provides a summary of the routes available to engineer the microstructures at the

Table 3
Summary of levels of microstructure engineering and effects on properties (ceramic system in parenthesis refers to example in text)

Level	Compositional change	Effect	Processing	Effect
Grain	Adjust bulk composition to give zero τ_ε	Improved temperature stability and increase or decrease in ε_r	Reduce porosity	Increased relative permittivity ε_r
			Anneal sample and develop surface phases	Beneficial surface phases help to increase Q (BZN)
			Chemical preparation of powder, in place of mixed oxide	Reduce impurities and increase Q ($MgTO_3$)
			Isostatic pressing versus uniaxial pressing	Lower internal stresses with isostatic pressing; higher Q ($MgTiO_3$)
			Non-interacting grains versus intimate fine powders in two component systems	Improved temperature stability (τ_ε) with large non-interacting granules (ATN)
Grain boundary	(ZTS) Add NiO to powder containing Fe_2O_3	NiO combines with Fe_2O_3 to form spinel phase in grain boundary, preventing Fe entering the grains and reducing Q	Leach powders to remove impurities	Less impurities in the grain boundary and bulk, higher Q (B2T9)
Sub-grain	Add '8-1-6-24' phase to BZN	Increase grain size; increase domain size; increase Q value (BZN)	($CaTiO_3$) anneal or cool slowly	Increase grain size, reduce density of domains; increase Q value ($CaTiO_3$)
Lattice	Acceptor doping of Ti-based ceramics	Prevents reduction of Ti (B2T9) and formation of oxygen vacancies; higher Q	Anneal or cool slowly	Increase cation ordering, increase Q value (complex perovskites and ZTS)
	Add cations of higher valency to powders containing impurities of lower valency than the host	Higher valency species compensate for lower valency impurities, preventing formation of oxygen vacancies (or electronic conduction) which would reduce Q (ZTS)		
	Introduce different cations into unit cell to adjust tolerance value t	Changes to t value modify the octahedral tilting and the τ_f value (complex perovskites)		

levels of the grain, the grain boundary, the sub-grain and the lattice. Adjustment to the relative permittivity can be achieved by reduction in porosity, and bulk changes to the composition. There are a variety of ways to increase the Q value; many relate to reducing impurity levels in the starting powder, and avoiding the presence of impurities in the grain boundaries and the primary grains. Equally important are reductions of local strain, reduction in the density of domains, and increasing cation ordering. To optimise the temperature stability of the dielectric two very different strategies were described. Where two component powder mixtures failed to provide the temperature stable performance (zero coefficient of ε_r) predicted by simple mixing rules, then large non-interacting grains were found to be successful. A more generally applicable way to achieve zero τ_f is to selectively introduce different cations into the unit cell to adjust the tolerance factor; this reflects changes in the octahedral tilting in the structure which in turn controls the τ_f value.

Acknowledgements

The authors acknowledge support from the EPSRC for work on microwave dielectric ceramics, including awards GR/R72655/01 and GR/T19148. We thank colleagues for support and access to previously unpublished material, particularly G. Ravi and Wenjin Wang.

References

1. Richtmyer, R. D., Dielectric resonators. *J. Appl. Phys.*, 1939, **10**, 391–398.
2. Bolton, R. L., PhD Thesis, University of Illinois, Urbana-Champaign, IL, 1968.
3. Kolar, D., Stadler, Z., Gabersek, S. and Suvorov, D., High stability, low loss dielectrics in the system $BaO–Nd_2O_3–TiO_2–Bi_2O_3$. *Ber. Deut. Keram. Ges.*, 1978, **55**, 346–350.
4. O'Bryan, H. M., Thompson, J. and Plourde, J. K., New $BaO–TiO_2$ compounds with temperature stable high permittivity and low dielectric loss. *J. Am. Ceram. Soc.*, 1974, **57**, 450–453.
5. Wakino, K., Nishikawa, T., Ishikawa, Y. and Tamura, H., Dielectric resonator materials and their application for mobile communication systems. *Br. Ceram. Trans. J.*, 1990, **89**(2), 39–43.
6. Cohn, S. B., Microwave bandpass filters containing high Q dielectric resonators. *IEEE Trans. MTT*, 1968, **MTT-16**, 218.
7. Reaney, I. M. and Iddles, D., Microwave dielectric ceramics for resonator and filters in mobile phone networks. *J. Am. Ceram. Soc.*, 2006, **89**, 2063–2072.
8. Gupta, T. K., Microstructural engineering through donor and acceptor doping in the grain and grain boundary of a polycrystalline ceramic. *J. Mater. Res.*, 1992, **7**, 3280–3295.
9. Negas, T., Yeager, G., Bell, S. and Amren, R., Chemistry and properties of temperature compensated microwave dielectrics, NIST Special Publication 804. In *Proceedings of the International Conference on Chemistry of Electronic and Ceramic Material, 1990*, 1991, pp. 21–34.
10. Plourde, J. K. and Ren, C.-L., Application of dielectric resonators in microwave components. *IEEE Trans. MTT*, 1981, **29**, 754–770.

11. Freer, R., Microwave dielectric ceramics—an overview. *Silic. Ind.*, 1993, **9–10**, 191–197.
12. Volkov, A. A., Gorshunov, B. P., Komandin, G., Fortin, W., Kugel, G. E., Kanai, A. and Grigas, J., High frequency dielectric spectra of $AgTaO_3$ $AgNbO_3$ mixed ceramics. *J. Phys. Condens. Matter*, 1995, **7**, 785–793.
13. Valant, M., Suvorov, D., Hoffmann, C. and Sommariva, H., Ag(Nb,Ta)O_3-based ceramics with suppressed temperature dependence of permittivity. *J. Eur. Ceram. Soc.*, 2001, **21**, 2647–2651.
14. Hughes, H., Azough, F. and Freer, R., Development of surfaces phases in $Ba(Zn_{1/3}Nb_{2/3})O_3$ ¯$Ba(Ga_{1/2}Ta_{2/3})O_3$ microwave dielectric ceramics. *J. Eur. Ceram. Soc.*, 2005, **25**, 2755–2758.
15. Ferreira, V. M., Azough, F., Baptista, J. L. and Freer, R., Proceedings of ECAPD-2 (London 1992). *Ferroelectrics*, 1992, **133**, 127–132.
16. Davies, P. K. and Roth, R. S., Defect intergrowths in barium polytitanates. I. $Ba_2Ti_9O_{20}$. *J. Solid State Chem.*, 1987, **71**, 490–502.
17. Wakino, K., Minai, K. and Tamura, H., Microwave characteristics of (Zr,Sn)TiO4 and BaO–PbO–Nd_2O_3–TiO_2 dielectric resonators. *J. Am. Ceram. Soc.*, 1984, **67**, 278–281.
18. Kipkoech, E. R., Azough, F. and Freer, R., Microstructural control of microwave dielectric properties in CaTiO3–La(Mg1/2Ti1/2)O3 ceramics. *J. Appl. Phys.*, 2000, **97**(6), 11, article no. 064103 (15 March).
19. Wang, Y. and Liebermann, R. C., Electron microscopy study of domain structure due to phase transitions in natural perovskite. *Phys. Chem. Miner.*, 1993, **20**, 147–158.
20. Lowe, T., Azough, F. and Freer, R., The microwave dielectric properties and structure of xCaTiO$_3$–$(1-x)$$Li_{0.5}Nd_{0.5}TiO_3$ ceramics. *J. Korean Ceram. Soc.*, 2003, **40**(4), 328–332.
21. Wakino, K., Murata, M. and Tamura, H., Far infrared reflection spectra of Ba(Zn,Ta)O_3–$BaZrO_3$ resonator material. *J. Am. Ceram. Soc.*, 1986, **69**, 34–37.
22. Spitzer, W. G., Miller, R. C., Kleinman, D. A. and Howarth, L. E., Far infrared dispersion spectra for $BaTiO_3$, $SrTiO_3$ and TiO_2. *Phys. Rev.*, 1962, **126**, 1710–1721.
23. Perry, C. H., McCarthy, D. J. and Rupprecht, G., Dielectric dispersion of some perovskite zirconates. *Phys. Rev.*, 1965, **138**, A1537–A1538.
24. Tamura, H., Sagala, D. A. and Wakino, K., Lattice vibrations of $Ba(Zn_{1/3}Ta_{2/3})O_3$ crystal with ordered structures. *Jpn. J. Appl. Phys.*, 1986, **25**, 787–791.
25. Petzelt, J., Pacesova, S., Fousek, J., Kamba, S. and Zeleny, V., Dielectric spectra of some ceramics for microwave applications in the range 1010–1014 Hz. *Ferroelectrics*, 1989, **93**, 77–85.
26. Gurevich, V. L. and Tagantsev, A. K., Intrinsic dielectric loss in crystals. *Adv. Phys.*, 1991, **40**, 719–767.
27. Kawashima, S., Nishida, J., Ueda, J. and Ouch, H. i, $Ba(Zn_{1/3}Ta_{2/3})O_3$ ceramics with low dielectric loss at microwave frequencies. *J. Am. Ceram. Soc.*, 1983, **66**(6), 421–423.
28. Tamura, H., Konoike, Y. T., Sakabe, Y. and Wakino, K., Improved high Q dielectric resonator with complex perovskite structure. *J. Am. Ceram. Soc.*, 1984, **67**(4), C59–C61.
29. Matsumoto, K., Hiuga, T., Takeda, K. and Ichimura, H., $Ba(Mg_{1/3}Ta_{2/3})O_3$ ceramics with ultra low loss at microwave frequencies. In *Proceedings of the Sixth IEEE International Symposium on Application of Ferroelectrics*, 1986, pp. 118–121.
30. Azough, F. and Freer, R., Microstructural development and microwave dielectric properties of $ZrTiO_4$-based ceramics. In *Proceedings of the Seventh IEEE International Symposium on Applications of Ferroelectrics, 1990*. IEEE, Piscataway, NJ, 1991, pp. 198–201.
31. Tamura, H., Microwave loss quality of $(Zr_{0.8}Sn_{0.2})TiO_4$. *Am. Ceram. Soc. Bull.*, 1994, **73**, 92–95.
32. Christofferson, R. and Davies, P. K., Extended defect intergrowths in $Zr_{1-x}Ti_{1+x}O_4$. *Solid State Ionics*, 1992, **57**, 59–69.
33. Templeton, A., Wang, X., Penn, S. P., Webb, S. J., Cohen, L. and Alford, N. M., Microwave dielectric loss of titanium oxide. *J. Am. Ceram. Soc.*, 2000, **83**, 95–100.
34. Nomura, S., Tomoya, K. and Kaneta, K., Effect of Mn doping on the dielectric properties of $Ba_2Ti_9O_{20}$ ceramics at microwave frequencies. *Jpn. J. Appl. Phys.*, 1983, **22**, 1125–1128.
35. Negas, T., Yeager, G., Bell, S., Coats, N. and Minis, I., $BaTi_4O_9$–$Ba_2Ti_9O_{20}$-based ceramics resurrected for modern microwave applications. *Am. Ceram. Soc. Bull.*, 1993, **72**, 80–89.
36. Iddles, D. M., Bell, A. J. and Moulson, A., Relationship between dopants, microstructure and the microwave dielectric properties of ZrO_2–TiO_2–SnO_2 ceramics. *J. Mater. Sci.*, 1992, **27**(23), 6303–6310.
37. Harrop, P. J., Temperature coefficient of capacitance of solids. *J. Mater. Sci.*, 1969, **4**, 370–374.
38. Colla, E. L., Reaney, I. R. and Setter, N., Effect of structural changes in complex perovskites on the temperature coefficient of relative permittivity. *J. Appl. Phys.*, 1993, **74**(5), 3414–3425.
39. Reaney, I. M., Colla, E. L. and Setter, N., Dielectric and structural characterisation of Ba- and Sr-based complex perovskite as a function of tolerance factor. *Jpn. J. Appl. Phys.*, 1994, **33**, 3984–3990.
40. Ravi, G., University of Manchester—from unpublished study.
41. Glazer, A. M., Simple ways of determining perovskite structures. *Acta Cryst.*, 1975, **A31**, 756–762.